THE JOURNAL OF BIOLOGICAL CHEMISTRY VOL. 281, NO. 38, pp. 28058–28067, September 22, 2006

ATP Regulation in Adult Rat Cardiomyocytes

*TIME-RESOLVED DECODING OF RAPID MITOCHONDRIAL CALCIUM SPIKING IMAGED WITH TARGETED PHOTOPROTEINS**[S]

Received for publication, May 11, 2006, and in revised form, July 10, 2006 Published, JBC Papers in Press, July 31, 2006, DOI 10.1074/jbc.M604540200

Christopher J. Bell[‡§], **Nicholas A. Bright**[¶], **Guy A. Rutter**[§‖**1], **and Elinor J. Griffiths**[‡§2]

From the [‡]*Bristol Heart Institute,* [‖]*Henry Wellcome Laboratories for Integrated Cell Signalling, the* [§]*Department of Biochemistry, University of Bristol, Bristol BS8 1TD, the* **Department of Cell Biology, Division of Medicine, Sir Alexander Fleming Building, Imperial College, Exhibition Road, London SW7 2AZ, and* [¶]*Cambridge Institute for Medical Research, Addenbrooke's Hospital, University of Cambridge, Cambridge CB2 2XY, United Kingdom*

The mechanisms that enable the heart to rapidly increase ATP supply in line with increased demand have not been fully elucidated. Here we used an adenoviral system to express the photoproteins luciferase and aequorin, targeted to the mitochondria or cytosol of adult cardiomyocytes, to investigate the interrelationship between ATP and Ca^{2+} in these compartments. In neither compartment were changes in free [ATP] observed upon increased workload (addition of isoproterenol) in myocytes that were already beating. However, when myocytes were stimulated to beat rapidly from rest, in the presence of isoproterenol, a significant but transient drop in mitochondrial [ATP] ($[ATP]_m$) occurred (on average to 10% of the initial signal). Corresponding changes in cytosolic [ATP] ($[ATP]_c$) were much smaller (<5%), indicating that $[ATP]_c$ was effectively buffered in this compartment. Although mitochondrial $[Ca^{2+}]$ ($[Ca^{2+}]_m$) is an important regulator of respiratory chain activity and ATP production in other cells, the kinetics of mitochondrial Ca^{2+} transport are controversial. Parallel experiments in cells expressing mitochondrial aequorin showed that the drop in $[ATP]_m$ occurred over the same time scale as average $[Ca^{2+}]_m$ was increasing. Conversely, in the absence or presence of isoproterenol, clear beat-to-beat peaks in $[Ca^{2+}]_m$ were observed at 0.9 or 1.3 μM, respectively, concentrations similar to those observed in the cytosol. These results suggest that mitochondrial Ca^{2+} transients occur during the contractile cycle and are translated into a time-averaged increase in mitochondrial ATP production that keeps pace with increased cytosolic demand.

Aerobic energy production in the heart is essential for the maintenance of normal contractility, but the mechanisms through which ATP homeostasis is achieved are incompletely understood. Early studies on isolated mitochondria showed that the main regulator of ATP production was likely to be ADP (1), so it seemed probable that this parameter had to increase, and ATP levels fall, before any stimulation of respiration occurred (reviewed by Brown (2)). However, subsequent studies using ^{31}P NMR in whole hearts showed that ATP levels were maintained during increased workload (3), implicating alternative regulatory mechanisms in the control of mitochondrial respiration. One such mechanism is provided by Ca^{2+}; in many mammalian cell types, changes in the free Ca^{2+} concentration in the mitochondrial matrix ($[Ca^{2+}]_m$),[3] by agonists that increase cytosolic free $[Ca^{2+}]$ ($[Ca^{2+}]_c$), stimulate ATP production by activating three mitochondrial dehydrogenases (4) and also possibly by activating the F_0F_1-ATPase (5, 6). However, the ability of $[Ca^{2+}]_m$ to increase ATP on a rapid time scale, as would have to occur in the heart to meet sudden changes in energy demand, has not been investigated, and exactly how ATP supply and demand are so well matched in the heart remains controversial even after over 40 years of research (7).

Another problem is that the mitochondrial Ca^{2+} transporters would have to respond very rapidly to increases in $[Ca^{2+}]_c$ in order to maintain constant ATP levels. Previous work on isolated mitochondria suggested that the mitochondrial Ca^{2+} uniporter (CaUP) was a relatively slow Ca^{2+}-uptake pathway, and the efflux pathway, the Na^+/Ca^{2+} exchanger (mNCX), was even slower (8, 9). So these pathways could certainly not respond quickly enough to the very rapid (millisecond) changes in $[Ca^{2+}]_c$ that occur during excitation-contraction coupling to achieve beat-to-beat regulation of $[Ca^{2+}]_m$. However, more recent work using isolated myocytes has suggested that mitochondrial Ca^{2+} transients do occur during excitation-contraction coupling (10), although there are conflicting data on this in the literature, because other studies reported that mitochondrial Ca^{2+} accumulation occurred over tens of seconds (11–13).

Such controversy, together with a resurgence of interest in the role of intramitochondrial Ca^{2+} in both cell signaling and the regulation of energy metabolism, has highlighted the need for methods that can be used to measure $[Ca^{2+}]_m$ dynamically and specifically in living cells. Most previous work attempting

* This work was supported by a British Heart Foundation project grant (to E. J. G. and G. A. R.) and a Wellcome Trust programme grant (to G. A. R.). The costs of publication of this article were defrayed in part by the payment of page charges. This article must therefore be hereby marked "*advertisement*" in accordance with 18 U.S.C. Section 1734 solely to indicate this fact.

[S] The on-line version of this article (available at http://www.jbc.org) contains supplemental Experimental Procedures, supplemental Results, and supplemental Refs. 1–3.

[1] A Wellcome Trust research leave fellow.

[2] To whom correspondence should be addressed: Department of Biochemistry, School of Medical Sciences, University of Bristol, Bristol, UK, BS8 1TD. Tel.: 117-9287502; Fax: 117-9288274; E-mail: Elinor.Griffiths@bristol.ac.uk.

[3] The abbreviations used are: $[Ca^{2+}]_m$, mitochondrial $[Ca^{2+}]$; $[Ca^{2+}]_c$, cytosolic free $[Ca^{2+}]$; $[ATP]_m$, mitochondrial [ATP]; $[ATP]_c$, cytosolic [ATP]; SR, sarcoplasmic reticulum; CaUP, Ca^{2+} uniporter; mNCX, Na^+/Ca^{2+} exchanger; cAq, cytosolically targeted aequorin; mAq, mitochondrially targeted aequorin; GFP, green fluorescent protein.

to measure $[Ca^{2+}]_m$ has used fluorescent indicators, and an evident problem with such studies is that the dyes may not localize exclusively to the mitochondrial compartment.

Similarly, although ATP has been measured in whole hearts, and now in animals and humans using noninvasive ^{31}P NMR (7), again only relatively slow responses were measured, and so it could not be determined whether ATP was varying beat-to-beat or during the time taken for mitochondria to accumulate Ca^{2+} to a level sufficient to activate the dehydrogenases. Although microinjection of luciferase into single cardiomyocytes has been reported (14), we did not find it possible to microinject our cells without damaging them. This study reported rapid depletion of (cytosolic) ATP levels in response to an uncoupler but did not report changes in response to physiological conditions or in response to normal cell contraction. Furthermore, free ATP levels have not been directly measured in different compartments of the living cardiomyocyte, and the relationship between mitochondrial [ATP] ($[ATP_m]$) and cytosolic ATP ($[ATP]_c$) is not known.

Recently, Robert *et al.* (15) expressed a mitochondrially targeted aequorin (16) in neonatal cardiomyocytes using the "FuGENE" transfection reagent and observed beat-to-beat mitochondrial Ca^{2+} transients with kinetics that were broadly similar to those observed in the cytosol. However, these findings have not been extended to adult cardiomyocytes because the latter are not amenable to transfection by conventional procedures. To investigate the relationship between ATP and Ca^{2+} in both mitochondrial and cytosolic compartments, we generated adenoviruses containing luciferase or aequorin targeted to either cytosol or mitochondria (17–19).

Parallel experiments were performed to determine whether ATP levels changed under conditions where $[Ca^{2+}]_m$ increased. Our results indicate that $[ATP]_c$ is extremely well buffered in myocytes, even under conditions where the cells were stimulated to beat rapidly in the presence of an adrenergic agonist to further increase ATP demand by the cell. However, an initial drop in $[ATP]_m$ was observed before it recovered to higher than resting values. We also observed beat-to-beat changes in $[Ca^{2+}]_m$, the amplitude of which was increased in the presence of an adrenergic agonist. Furthermore, although the peak amplitude of the transient increased immediately upon rapid stimulation, there was an underlying level of $[Ca^{2+}]_m$ that increased more slowly. Together, these results suggest that changes in $[Ca^{2+}]_m$ may be translated time-dependently into steady-state alterations in free mitochondrial and, subsequently, cytosolic [ATP].

EXPERIMENTAL PROCEDURES

Materials—All materials were from Sigma or BDH (distributed by VWR International Ltd., Poole, UK) unless stated otherwise.

Myocyte Isolation and Culture—Adult male Wistar rats (250 g) were humanely killed by a blow on the head followed by cervical dislocation, and the heart was excised and placed into ice-cold modified Krebs Buffer (MKB) (in mM: 4.2 Hepes, pH 7.6, 130 NaCl, 5.4 KCl, 1.4 $MgCl_2$, 0.4 NaH_2PO_4, 10 glucose, 20 taurine, 10 creatine) containing 0.75 mM $CaCl_2$. Ca^{2+}-tolerant adult myocytes were then isolated by a Langendorf perfusion method (20) and were cultured on laminin-coated (5 μg/ml) dishes in Medium 199 containing penicillin (100 units/ml) and streptomycin (100 μg/ml). The cells were allowed to adhere for 4 h at 37 °C in an atmosphere of 5% CO_2, and then fresh medium was added.

Measurement of Mitochondrial and Cytosolic [ATP] Using Targeted Luciferase—Myocytes were cultured for 24 h in the presence of adenoviruses encoding either cytosolically or mitochondrially targeted luciferase at an multiplicity of infection of 50–100 (17). This time provided optimum expression of luciferase, since longer periods in culture with the luciferase viruses led to clear decreases in cell viability. One hour prior to recording, the cells were transferred into MKB, and 1 mM luciferin was added 1–2 min before recording. Culture dishes were placed on the stage of an Olympus IX-70 inverted microscope, and experiments were performed at 37 °C. Light emission from luciferase was detected in time-resolved imaging mode (60 frames s^{-1}) using a triply intensified charge coupled camera (ICCD218; Photek, Lewes, East Sussex, UK) (21). Light was detected from an entire field of view (typically 50–100 cells), using a −10 objective. Smoothing of traces was performed off-line using Microsoft Excel (18, 19), and images generated over an appropriate integration period.

Measurement of Mitochondrial and Cytosolic [Ca^{2+}] Using Targeted Aequorin—Myocytes were cultured as above for 48 h in the presence of adenoviruses encoding either cytosolically or mitochondrially targeted aequorin (cAq and mAq, respectively), at a multiplicity of infection of 50–100 (19). This period in culture was necessary for sufficient expression of aequorin and did not result in loss of cell viability, unlike the luciferase viruses. The adenoviruses also encoded untargeted green fluorescent protein (GFP). 1 h before experiments, myocytes were transferred to Ca^{2+}-free MKB containing 5 μM coelenterazine to reconstitute aequorin. Adult cells were stimulated electrically, and light emission from aequorin was detected at 37 °C, as above. Free $[Ca^{2+}]$ was calculated using the ratio of the counts at a specific time point to the total number of counts detected. This was determined by permeabilization of the cells to consume unused aequorin in the presence of digitonin (2–5 mg/ml) and 10 mM $CaCl_2$ (21). Dying cells, identified by sudden bursts of light because of essentially instantaneous aequorin consumption, were eliminated from further analysis.

Immunocytochemistry—Immunocytochemistry was performed as described (22). Briefly, infected cells were fixed in 4% paraformaldehyde and permeabilized with 0.5% Triton X-100. Goat polyclonal anti-luciferase (Promega, Madison, WI) or mouse monoclonal anti-hemagglutinin tag antibody (Covance Research Products, Berkeley, CA) was used at 1:50 in phosphate-buffered saline containing 1% bovine serum albumin and revealed with an Alexa 568-conjugated secondary antibody (Molecular Probes, 1:500 dilution) using a Leica TCS-NT confocal microscope (×63 objective).

Electron Microscopy—Immunoelectron microscopy was performed as described (23). Briefly, cells were washed in phosphate-buffered saline and fixed in 8% paraformaldehyde, 250 mM Hepes, pH 7.2, for 1 h at room temperature prior to embedding in gelatin and infusion with sucrose. Sections were cut on a Reichert Ultracut S ultramicrotome with a cryochamber

attachment (Leica, Milton Keynes, UK) and observed on a Philips CM 100 transmission electron microscope (Philips Electron Optics, Cambridge, UK). Ultrathin cryosections were indirectly labeled as described (23). Grids were incubated with primary antibody (1:100 mouse monoclonal anti HA) for 1 h at room temperature before detection with goat anti-mouse IgG 10 nm gold conjugate.

Statistics—Statistical significance was calculated using paired or unpaired Student's *t* tests, as appropriate.

RESULTS

Measurement of Mitochondrial and Cytosolic ATP Using Luciferase in Adult Myocytes—Targeted luciferases, introduced into myocytes by means of an adenoviral expression system, were used to monitor changes in [ATP] in both mitochondria and cytosol in living cells. The correct localization of the luciferase enzymes was confirmed by immunofluorescence studies using antibodies directed against luciferase (Fig. 1, *A* and *B*). Mitochondrially targeted luciferase (modified to include the amino-terminal leader sequence to cytochrome *c* oxidase subunit VIII) showed a restricted distribution (Fig. 1*A*), with no fluorescence in the cell nuclei and enhanced fluorescence around the periphery of the nuclei, consistent with a mitochondrial localization as expected (17, 18). In contrast, untargeted (cytosolic) luciferase was found throughout the cell, including the cell nuclei (Fig. 1*B*). Characteristic cytosolic or mitochondrial localization patterns were also seen in neonatal myocytes (see Supplemental Material).

To investigate whether there are any changes in ATP in either cytosol or mitochondria upon changes in ATP demand by the cell, adult myocytes were infected with adenoviruses encoding cytosolically or mitochondrially targeted luciferase; cells were then paced to beat by electrical stimulation at 2 Hz, before being subjected to an increase in workload induced by addition of the β-adrenergic agonist isoproterenol. No significant changes in apparent free [ATP] (other than those that could be reproduced by mock additions and were thus considered artifacts), either in cytosol or mitochondria, were observed upon addition of isoproterenol (Fig. 1, *C* and *D*) or upon transition to either an increased extracellular [Ca^{2+}] or increased stimulation rate (data not shown). In addition, no changes in $[ATP]_m$ were observed beat-to-beat (Fig. 1, *E* and *F*). $[ATP]_m$ did, however, change when myocytes were stimulated to beat from a resting state in the presence of isoproterenol, giving a large increase in workload. Under these conditions $[ATP]_m$ dropped initially by ~10% over 30–60 s. This drop was followed by a slower recovery to give a sustained rise in $[ATP]_m$ (Fig. 2, *A* and *C*). $[ATP]_m$ then returned to initial levels when the electrical stimulus was removed. This pattern was apparent when either glucose (Fig. 2*A*) or the mitochondrial substrates pyruvate and lactate (Fig. 2*C*) were used as fuels; the latter were used to enhance the likely contribution of mitochondrial ATP synthesis to overall changes in cellular [ATP]. No significant difference in magnitude of either the initial drop or the sustained rise between the two fuels was observed (Table 1). $[ATP]_c$ showed much smaller changes in response to increased work rate with either fuel (Fig. 2, *B* and *D*; Table 1).

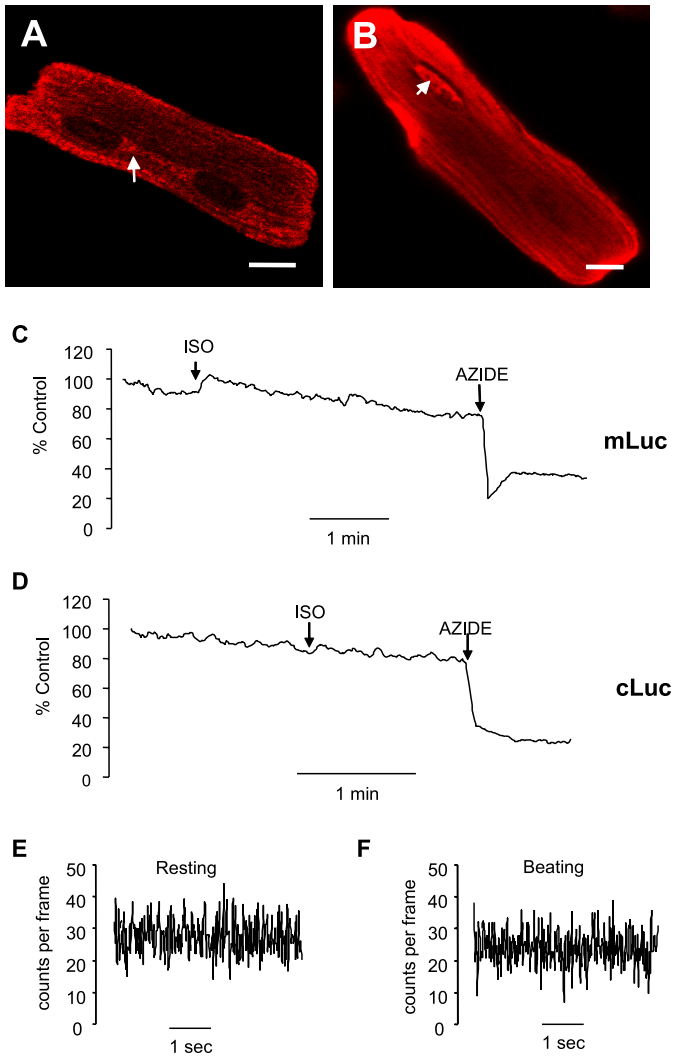

FIGURE 1. **Lack of detectable ATP changes in response to increased workload in already beating myocytes or during the contraction cycle.** *A* and *B*, to determine the localization of the luciferase probes, immunocytochemistry was performed using antibodies against luciferase in cells expressing either mitochondrially targeted luciferase (*mLuc*) (*A*) or cytosolically targeted luciferase (*cLuc*) (*B*). Imaging was then performed using confocal fluorescence microscopy. *Scale bars* represent 10 μm, and *arrows* show areas of interest. *C* and *D*, adult rat myocytes expressing either mitochondrially targeted (*C*) or untargeted luciferase (*D*) were allowed to beat in the presence of 2 mM extracellular Ca^{2+} at a rate of 2 Hz before the addition of 10 μM isoproterenol (*Iso*) where indicated. 20 mM sodium azide was then added where indicated to deplete ATP levels. Light output was integrated over 1 s. *E* and *F*, an average 5-s period from cells that were either resting (*E*) or beating at 2 Hz (*F*) (light output integrated every 1/60 s).

Measurement of [Ca^{2+}] Changes—Because $[Ca^{2+}]_m$ is considered to be an important signal regulating ATP production in mitochondria (4, 24), targeted aequorin molecules were used to monitor mitochondrial and cytosolic [Ca^{2+}] under similar conditions of large increases in workload. The localization of aequorin was confirmed by immunofluorescence and immunoelectron microscopy techniques using antibodies against the HA tag present on the aequorin molecule. Because the aequorin virus constructs also contained GFP expressed from a separate cytomegalovirus promoter (thus being untargeted) the aequorin distribution could also be compared with the GFP distribution. Mitochondrially targeted aequorin showed a similar distribution to mitochondrially targeted luciferase (Fig.

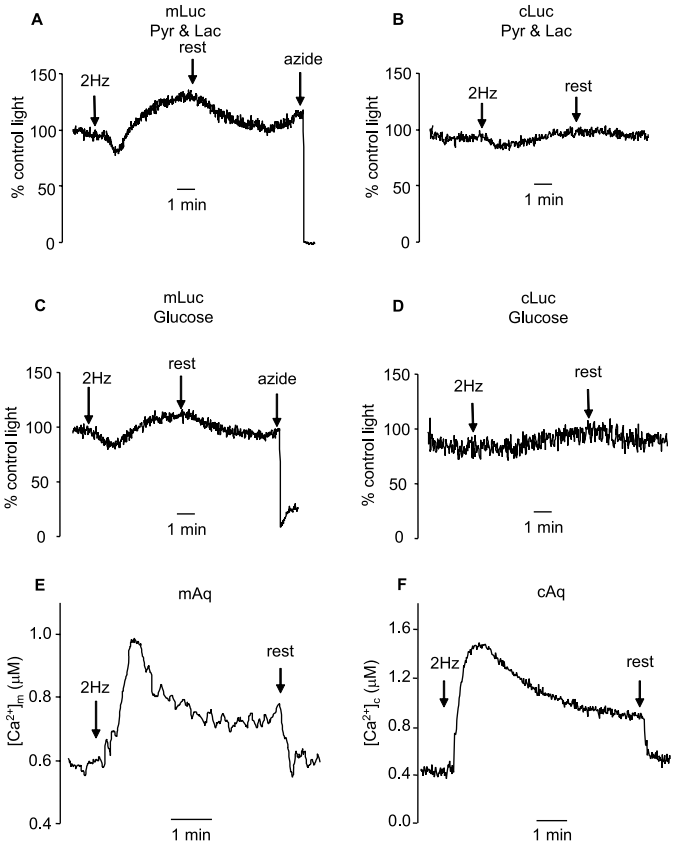

FIGURE 2. **Changes in mitochondrial and cytosolic [Ca^{2+}] and [ATP] measured during step changes in workload.** Myocytes were exposed to 10 μM isoproterenol while at rest and then stimulated at 2 Hz for several minutes (*1st arrow*) before being returned to rest (*2nd arrow*). *A–D,* myocytes expressing luciferase targeted to either mitochondria (*A* and *C*) or untargeted (*B* and *D*) were transferred to MKB containing either 10 mM pyruvate (*Pyr*) and 5 mM lactate (*Lac*) (*A* and *B*) or 10 mM glucose (*C* and *D*) at least 1 h prior to recording. The amount of light emitted is expressed relative to the amount of light emitted by the cells at rest at the beginning of each experiment. Luciferase light output was integrated over a 1-s period. *E* and *F*, myocytes expressing mitochondrially targeted (*E*) or untargeted (*F*) aequorin were used to measure [Ca^{2+}] in each compartment over the course of the experiments. Aequorin light output was integrated every second. *A–F*, each trace is representative of at least three similar experiments. Mean data are presented in Table 1.

TABLE 1

Percentage change in ATP observed in different compartments upon rapid stimulation of myocytes from rest

Experiments were performed as described in Fig. 4, and the % initial fall and subsequent rise in ATP-dependent light emission above base line were recorded under each condition as shown. Numbers in parentheses represent the number of separate fields of view studied, from at least three separate cell preparations. * indicates $p < 0.05$ *versus* corresponding figure using mitochondrially targeted luciferase (mLuc) (*t* tests). cLuc indicates cytosolically targeted luciferase; Pyr indicates pyruvate and Lac indicates lactate.

	mLuc		cLuc	
	Glucose	Pyr and Lac	Glucose	Pyr and Lac
ATP fall	9.2% ± 1.6 (9)	13.9% ± 2.4 (7)	2.0% ± 0.9 (7)*	4.0% ± 2.3 (3)*
ATP rise	19.7% ± 4.8 (9)	28.4% ± 5.0 (7)	8.9% ± 3.3 (7)*	5.0% ± 2.5 (3)*

3*A*), with no fluorescence in the nuclei and enhanced fluorescence in the perinuclear regions. This distribution was in marked contrast to both GFP and untargeted (cytosolic) aequorin (Fig. 3, *B, E,* and *F*), which was distributed throughout the cell, including the nuclei. GFP was also absent from the perinuclear regions (Fig. 3*B*), suggesting exclusion from the mitochondria. In addition, immuno-EM studies showed

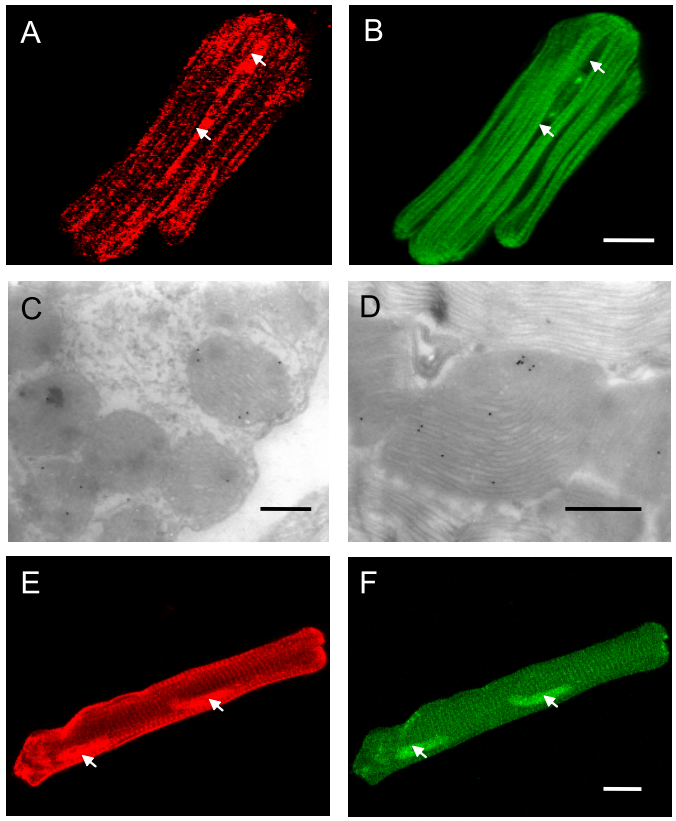

FIGURE 3. **Subcellular localization of targeted aequorin.** Adult rat myocytes were infected with adenoviruses encoding mitochondrial (*A–D*) or cytosolic (*E* and *F*) aequorin. Confocal fluorescence microscopy was performed to detect antibodies against the HA-tagged aequorin construct (*A* and *E*) as well as intrinsic GFP (co-expressed from viral vector) fluorescence (*B* and *F*). Electron microscopy was also performed to detect antibodies against the HA tag (*C* and *D*). From eight such EM images, ~90% (100/110) of the spots were mitochondrially localized. *Scale bars* represent 10 μm (images *A, B, E,* and *F*), 500 nm (*C*), or 200 nm (*D*). *Arrows* show areas of interest where aequorin fluorescence was concentrated but GFP fluorescence was low (*A* and *B*), or show nuclei (*E* and *F*).

~90% localization to the mitochondria (Fig. 3, *C* and *D*). Immunofluorescence studies of mAq and cAq in neonatal myocytes also showed characteristic distributions (see Supplemental Material).

Given that even a limited mislocalization of mAq to a nonmitochondrial site might significantly interfere with calculations of [Ca^{2+}] in this compartment, we also determined the fraction of mistargeted aequorin by additional, more quantitative methods. First, we determined the fraction of aequorin released upon selective permeabilization of cells with digitonin, saponin, or α-hemolysin (α-toxin) in "intracellular buffer." The mitochondrial Ca^{2+} uniporter inhibitor Ru360 was added to prevent mitochondrial Ca^{2+} uptake, along with 10 μM Ca^{2+} to fully activate any nonmitochondrial aequorin. Initial experiments using mAq-infected cells indicated that 24.4 ± 3.4% ($n = 20$) of the total light output was emitted at low concentrations of digitonin or 15 ± 1.08% ($n = 11$) in the presence of α-toxin. To determine whether mAq light output correlated with release of a mitochondrial marker enzyme (citrate synthase), we permeabilized cells with a low concentration of saponin (1 μg/ml). Even this concentration caused some release of citrate synthase, con-

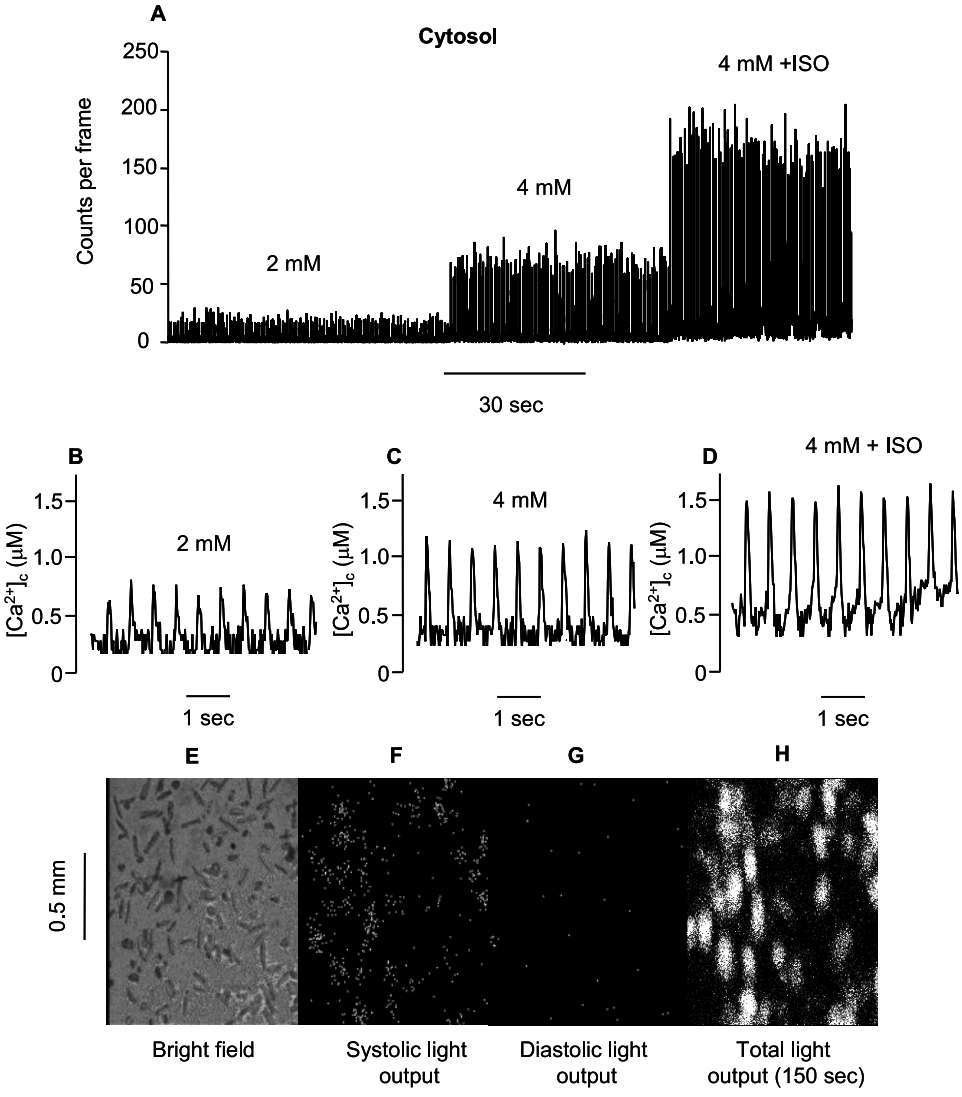

FIGURE 4. **Changes in $[Ca^{2+}]_c$ in contracting adult myocytes.** *A,* representative trace of the time course of light output from cytosolic aequorin. Cells were stimulated to beat at 2 Hz in 2 mM extracellular $CaCl_2$ for 60 s before the addition of a further 2 mM $CaCl_2$ from 60 to 110 s and finally the addition of 10 μM isoproterenol (*Iso*) from 110 to 150 s. *B–D,* $[Ca^{2+}]_c$ in this experiment over sample 5-s time frames for each condition. *E–H,* field of view of adult myocytes under ×10 magnification. *E,* bright field; *F,* light output detected by the camera during a 0.1-s period during which the cells contracted; *G,* light output detected by the camera during a 0.1-s period during which the cells did not contract; *H,* total light output detected by the camera over a 150-s period during which the cells were beating at 2 Hz.

firming that low concentrations of either saponin or digitonin are likely to damage intracellular membranes and contribute to the slightly higher estimates for mitochondrial mistargeting obtained using the detergents compared with α-toxin. However, by comparing the amount of citrate synthase activity released by saponin with mAq light output, it could be calculated that 82 ± 2% (n = 4) of aequorin was localized to mitochondria, in line with the value of 85% obtained using α-toxin. Full details of these experiments and their analysis are given in the Supplemental Material.

When cells were stimulated from rest in the presence of isoproterenol, large increases in $[Ca^{2+}]$ were observed in both cytosol and mitochondria (Fig. 2, *E* and *F*), peaking at ~40 s. $[Ca^{2+}]$ then decreased gradually to a lower steady-state level after ~60–90 s, the time scale of the increase in $[Ca^{2+}]$ therefore paralleling the decrease in [ATP] in both compartments. $[Ca^{2+}]_m$ and $[Ca^{2+}]_c$ both returned to base line when electrical stimulation ceased.

Detection of Beat-to-Beat Ca^{2+} Transients in Adult Cardiomyocytes—Beat-to-beat mitochondrial calcium transients have been observed previously in populations of neonatal rat myocytes (15) using targeted aequorin, and so it was interesting to determine whether these could also be detected in adult myocytes.

Having used the adenovirally expressed aequorin system to achieve similar results to those reported previously in neonatal myocytes (see Supplemental Material), we monitored changes in $[Ca^{2+}]$ using the same system in adult ventricular myocytes. In cAq-expressing cells, beat-to-beat changes in free $[Ca^{2+}]_c$ could easily be visualized (Fig. 4) in a cell population (10–100 cells), although they were close to the limit of detection at the single cell level. However, the amount of light at each systolic peak was much smaller than that observed in neonatal myocytes, as was the total amount of light released on addition of high concentrations of digitonin (not shown) indicating that expression was lower in these cells. No Ca^{2+} transients were ever observed in resting cells (in over 20 fields of cells studied (not shown)).

In mAq-expressing cells, the total light output (assessed as described above) was very small compared with that in experiments using cAq. This limitation made it difficult to observe changes in $[Ca^{2+}]$ at normal (1–2 mM) extracellular $[Ca^{2+}]$, because even systolic $[Ca^{2+}]_m$ peaks gave a minimal increase in photon production and hence were close to the limit of detection. The reasons for the less efficient expression of mAq *versus* cAq (also observed in neonatal myocytes) are unclear; however, beat-to-beat Ca^{2+} transients were clearly observed at higher extracellular $[Ca^{2+}]$ (4 mM) or in the presence of isoproterenol (Fig. 5). Again, no Ca^{2+} transients were ever observed in resting cells (15 separate experiments). The time course for mitochondrial and cytosolic transients is compared in Fig. 5*D*, whereas the initial phase of the upstroke of the mitochondrial transient is qualitatively very similar to that of the cytosolic, and the down stroke appears to lag behind, indicating a slower mitochondrial Ca^{2+} efflux. The recording

time scale possible with aequorin is unfortunately not fast enough to allow accurate quantification of these kinetics.

Although diastolic $[Ca^{2+}]$ could not be accurately determined in either compartment because of very low light output at these low $[Ca^{2+}]$ (<0.2 μM), peak systolic $[Ca^{2+}]_m$ and $[Ca^{2+}]_c$ could be measured and were similar at ~0.9 μM, a value that rose upon a further increase of extracellular calcium or the addition of isoproterenol (Table 2 and Figs. 4 and 5). The effect of isoproterenol was more pronounced in adult cells than in neonatal cells with peak systolic concentrations of ~1.6 and 1.2 μM, respectively (Table 2). The diastolic concentration of both $[Ca^{2+}]_m$ and $[Ca^{2+}]_c$ also appeared to increase upon addition of isoproterenol (Figs. 4 and 5), although this could not be accurately quantified (see above).

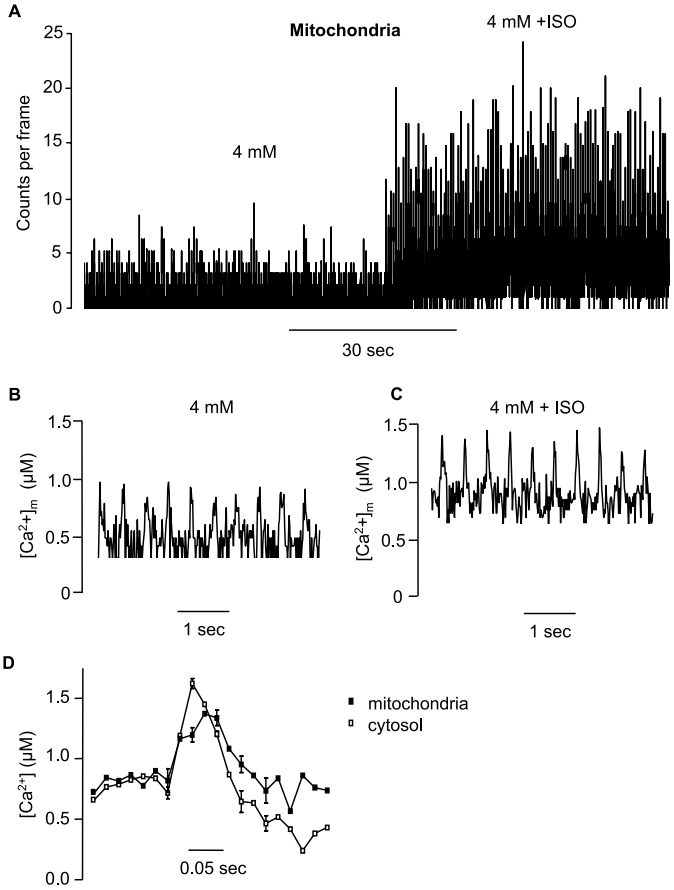

FIGURE 5. **Changes in $[Ca^{2+}]_m$ in contracting adult myocytes.** *A*, representative trace of the time course of light output from the mitochondrially targeted aequorin; cells were stimulated at 2 Hz in 4 mM extracellular $CaCl_2$ for 60 s before the addition of 10 μM isoproterenol (*Iso*) for a further 60 s. *B* and *C*, $[Ca^{2+}]_m$ in this experiment over a sample 5-s time frame for each condition. *D*, comparison of mitochondrial and cytosolic Ca^{2+} transients from single cells over a rapid timescale.

We are confident that the mitochondrial Ca^{2+} transients observed do in fact originate largely from the mitochondria; if all of the systolic light output were due to mAq in the cytosol, then the $[Ca^{2+}]$ values we observed would have required a 60% mistargeting of mAq, greatly in excess of our actual mistargeting of 15%. Full details of this theoretical calculation are given in the Supplemental Material. Using a similar calculation (not shown), we estimate that the mistargeting of mAq to the cytosol leads to only a small (≤7%) underestimate of the $[Ca^{2+}]_m$ spike amplitude.

Inhibition of Mitochondrial Ca^{2+} Transport—To investigate whether inhibition of mitochondrial Ca^{2+} transport might affect cytosolic Ca^{2+} signaling, we attempted to inhibit these pathways in living cells. Clonazepam is an inhibitor of the mNCX, the main mitochondrial Ca^{2+}-efflux pathway in the heart, and does not affect L-type Ca^{2+} channels, Ca^{2+} transporters of the sarcoplasmic reticulum (SR) (25–27), or cell contraction (28, 29). We have previously attempted to use CGP37147, which inhibits the mNCX in isolated mitochondria, but we found that it could not be used effectively in living cardiomyocytes, as it did not consistently inhibit the mNCX (28). Here, clonazepam eliminated mitochondrial Ca^{2+} transients but produced a pronounced and sustained elevation of $[Ca^{2+}]_m$ (Fig. 6, *A1* and *A2*). This increase in $[Ca^{2+}]_m$ occurred gradually over the course of ~60 s (Fig. 6*A2*) and thus may represent a gradual build up of $[Ca^{2+}]_m$ by a succession of individual spikes before reaching a plateau. Systolic Ca^{2+} transients, by contrast, remained in the cytosol but with reduced amplitude (Fig. 6*B*). To exclude the possibility that clonazepam was inhibiting cytosolic Ca^{2+} transients in a subset of cells (which could also account for these results), we recorded data from a single cell (Fig. 6*C*); this shows almost exactly the same changes as those of the mean population.

Although we attempted to inhibit mitochondrial Ca^{2+} uptake via the mitochondrial CaUP with Ru360, this drug did not appear to be cell-permeant in our hands, in agreement with the findings of Robert *et al.* (15). We also tried adding a mitochondrial uncoupler (carbonyl cyanide *p*-trifluoromethoxyphenylhydrazone) with oligomycin, which should dissipate the mitochondrial membrane potential but not affect $[ATP]_m$ significantly in the short term (see Supplemental Material). Examined in the cytosol we found that although $[Ca^{2+}]_c$ transients remained, in many experiments they were significantly reduced (details given in Supplemental Material). Although we never observed mitochondrial Ca^{2+} transients in the presence of oli-

TABLE 2

Peak systolic $[Ca^{2+}]_m$ and $[Ca^{2+}]_c$ in adult and neonatal cardiomyocytes

Myocytes were exposed to varying external $[Ca^{2+}]$ in the absence or presence of 10 μM isoproterenol (ISO). Numbers in parentheses indicate the number of fields of view studied, from at least three separate cell preparations. * indicates $p < 0.05$ *versus* 2 mM calcium; # indicates $p < 0.05$ *versus* condition in the absence of isoproterenol (paired *t* tests).

Adult			Neonate		
External $[CaCl_2]$	cAq	mAq	External $[CaCl_2]$	cAq	mAq
mM	μM		mM	μM	
2	0.89 ± 0.04 (36)	0.90 ± 0.09 (11)	2	0.84 ± 0.07 (13)	0.83 ± 0.07 (9)
4	1.14 ± 0.10 (14)*	1.00 ± 0.09 (14)*	4	0.94 ± 0.07 (11)*	1.09 ± 0.06 (5)*
2 + ISO	1.65 ± 0.07 (19)#	1.23 ± 0.11 (10)#	2 + ISO	0.98 ± 0.10 (3)#	0.92 ± 0.10 (3)#
4 + ISO	1.46 ± 0.11 (9)#	1.35 ± 0.06 (15)#	4 + ISO	1.23 ± 0.09 (8)#	1.28 ± 0.16 (3)#

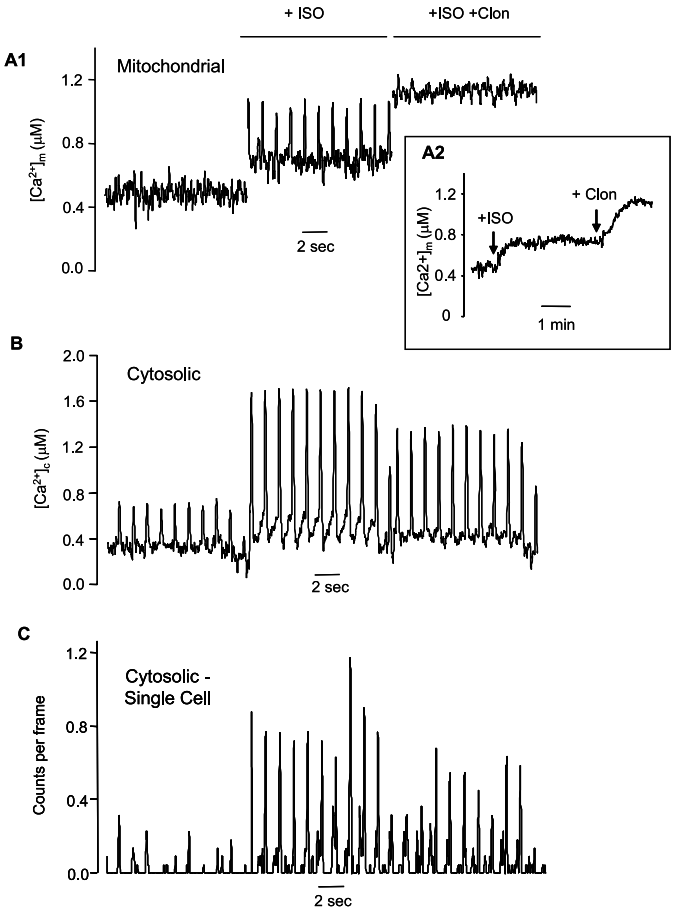

FIGURE 6. **Effect of clonazepam on mitochondrial and cytosolic calcium transients.** Adult myocytes expressing either mitochondrial (*A1* and *A2*) or cytosolic (*B* and *C*) aequorin were stimulated to beat in the presence of 2 mM extracellular $[Ca^{2+}]$. Isoproterenol (*ISO*) was added after 60 s, followed by 50 μM clonazepam (*Clon*) after 300 s. *A1*, *B*, and *C* represent a 10-s period under each condition, which is the overlaid average of four continuous 10-s periods under that condition integrated every 1/60 s. *A2* represents the entire time span of the experiment shown in *A1* integrated every second in order to show how Ca^{2+} changes upon addition of isoproterenol and clonazepam. *A1*, *A2*, and *B* represent data from a field of cells; *C* represents the counts measured from one single cell within the field shown in *B*. These data are representative of at least three separate experiments. Mean peak systolic $[Ca^{2+}]$ values (μM) in the presence and absence of clonazepam are as follows: $[Ca^{2+}]_c$, control (no additions) 1.02 ± 0.02 (10); *, $p < 0.01$ *versus* condition in absence of clonazepam (Student's *t* test); isoproterenol only, 1.91 ± 0.09 (8); isoproterenol and clonazepam, 1.48 ± 0.09* (10); $[Ca^{2+}]_m$, isoproterenol only, 1.22 ± 0.07 (14); isoproterenol and clonazepam (nonoscillating), 1.23 ± 0.08 (14). *Numbers* in *parentheses* represent the number of individual experiments performed.

gomycin and carbonyl cyanide *p*-trifluoromethoxyphenylhydrazone, suggesting that Ca^{2+} entry into mitochondria was indeed inhibited, from these experiments we could not rule out the possibility that a lower $[Ca^{2+}]_m$ was secondary to a reduced $[Ca^{2+}]_c$.

DISCUSSION

The principal aim of this study was to investigate the relationship between [ATP] and $[Ca^{2+}]$ in the cytosol and mitochondria in fully differentiated single adult cardiac myocytes. To achieve this we used a high sensitivity photon counting system to image luciferase (18, 19, 30) or aequorin (21) targeted to either the cytosol or mitochondrial matrix. We found that adenoviral vectors can be used as effective vehicles for both photoproteins, with ~85% targeting efficiency, and that photon-counting imaging of bioluminescence can be used to monitor [ATP] and $[Ca^{2+}]$ in small populations (10–100) of cells. Thus, although this approach did not readily allow Ca^{2+} imaging at the single cell level because of the relatively poor photon production of the bioluminescent reporters, we found that it permitted measurements of mitochondrial Ca^{2+} that were relatively unaffected by changes in intramitochondrial pH or cell contraction. By contrast, these factors severely confounded attempts to measure mitochondrial Ca^{2+} in adult cardiac myocytes using the recently developed molecularly targeted fluorescent probe, "pericam" (31, 32).[4]

Our results demonstrate the following: (*a*) $[ATP]_c$ is effectively buffered under physiological conditions even upon sudden increases in energy demand; (*b*) when myocytes are suddenly stimulated to beat rapidly from rest, there is an initial drop in $[ATP]_m$ before it rises again, corresponding to the time course for a steady-state increase in $[Ca^{2+}]_m$; (*c*) Ca^{2+} transients are likely to occur beat-to-beat within the matrix of mitochondria of adult cardiac myocytes with similar amplitude to those in the cytosol; and (*d*) inhibiting mitochondrial Ca^{2+} efflux causes significant changes in both mitochondrial and cytosolic Ca^{2+} homeostasis.

Regulation of ATP Supply in Response to Changes in Workload—We expressed luciferase in adult cardiomyocytes in order to measure $[ATP]_c$ or $[ATP]_m$. Although this technique does not readily allow calibration of ATP levels, changes in luciferase luminescence can nonetheless be taken as a reasonable guide to alterations in free [ATP] (18, 19). Used here in adult cardiac myocytes, this approach revealed no observable beat-to-beat changes (*i.e.* >1%) in free [ATP] in either cytosol or mitochondria. Moreover, no changes were observed upon addition of isoproterenol to cells that were already beating, suggesting that ATP supply is well matched to the increased demand caused by the isoproterenol-induced increase in contractile force. However, when we allowed cells to rest and then suddenly stimulated them to contract in the presence of isoproterenol, $[ATP]_m$ showed a significant transient drop (up to 22% in some cells) followed by recovery to higher than initial levels. These changes seem likely to reflect an initial activation of ATP-requiring processes in the cytosol, such as ion pumps and contractile proteins, which would causes a drop in $[ATP]_m$ before a time-dependent activation of mitochondrial oxidative metabolism by Ca^{2+} (17, 19) stimulated ATP synthesis. Rapid Ca^{2+} uptake by the CaUP could also cause a transient decrease in mitochondrial membrane potential, which would limit ATP supply; however, whether this occurs *in vivo* during a single contraction is not known but has not been observed using fluorescent indicators like JC-1 or rhodamine 123 (33, 34). The changes in $[ATP]_c$ were much smaller than those in the mitochondrial matrix, again suggesting that even when $[ATP]_m$ does change, the cytosolic energy supply is very rapidly matched to the increased demand.

To our knowledge, this is the first study to measure such rapid changes in [ATP] in cardiac cells or muscle. Others have

[4] C. J. Bell and G. A. Rutter, unpublished data.

used measurements of NAD(P)H levels in whole hearts (35, 36), myocytes (37), or trabeculae (38) as an indirect indicator of increases in the rate of ATP synthesis. Moreover, several studies have concluded that when cells or whole hearts are excited with ultraviolet light, 90% of cellular autofluorescence originates from NADH in mitochondria (39, 40). One problem with this is that any change in oxygen tension will tend to increase NAD(P)H due to inhibition of respiration (7). However, in well oxygenated hearts, no change in NADH was observed in response to physiological increases in workload (36). Additionally, altering the substrate from glucose to pyruvate did increase NADH, and this was associated with an increase in the ATP/ADP + P_i and increases in O_2 consumption (41). However, although lactate gave the same increased NADH, there was no rise in ATP/ADP + P_i. So similar levels of NADH were associated with different ATP/ADP + P_i, and so an increase in NADH cannot be taken as an unambiguous indicator of increased ATP production (41).

In myocytes, conflicting results have been obtained as to whether NADH changes upon rapid stimulation of cells, and increases, no change, and decreases have all been reported (28, 37, 42). In isolated trabeculae, NADH was more carefully measured by using an internal reference that negated motion artifacts. When the muscle strips were stimulated at 3 Hz from rest, an initial drop in $NADH_{max}$ within 5 s followed by an increase to initial or higher levels over 60 s was observed (43). This is almost exactly what we observed with ATP levels, and the conditions are the most similar to our experiments, namely that the muscle cells were stimulated to beat from rest. No experiments were performed where an adrenergic agonist was added to cells already stimulated to beat, as in our experiments.

Stimulation of ATP Synthesis by Ca^{2+}—If ATP levels are falling, and presumably ADP rising, during the initial few seconds, then ADP could provide the stimulation of ATP synthesis required to keep $[ATP]_c$ relatively constant during this period. Also, the average $[Ca^{2+}]_m$ takes 30–60 s to reach its maximum value (Fig. 2) and so again would not stimulate dehydrogenases and NADH production during the initial phase. Only after this occurred would $[ATP]_m$ increase again. An almost identical time course for changes in $[Ca^{2+}]_m$ in response to rapid stimulation has been reported using the isolated trabeculae model described above (29). Additionally, when muscle work was increased without increases in $[Ca^{2+}]$, no recovery of the NADH signal occurred (43), again suggesting that $[Ca^{2+}]_m$ is essential for this phase. An important caveat must, however, be made that because we compared changes in ATP with luciferase and Ca^{2+} with aequorin, after 1 or 2 days of culture, respectively, there may be subtle changes in cell physiology between these two time points that might affect the changes in these two parameters following cell stimulation.

The increase in ATP demand is produced by the contractile apparatus and ion pumps, which together account for over 70% of ATP consumption by cardiac myocytes (44). The increased ATP usage would result in decreased ATP and increased ADP; however, metabolic buffering by the creatine kinase system would maintain $[ATP]_c$ for a few seconds, allowing ADP to be rapidly and preferentially channeled into the mitochondria in exchange for ATP on the adenine nucleotide translocase. Stimulation of oxidative phosphorylation by ADP would then maintain $[ATP]_c$ at the expense of $[ATP]_m$, until the supply of reducing equivalents stimulated by $[Ca^{2+}]_m$ activation of the dehydrogenases has caught up.

However, the above only explains observations about what happens when cells, trabeculae, or hearts are subjected to sudden, large increases in workload. As shown in Fig. 1, when cells are already beating rapidly, there is no change on addition of isoproterenol despite an increase in cell contraction, and hence in ATP demand. Similarly, physiological increases in workload in whole hearts did not result in any increase in NAD(P)H (36).

In cells and hearts that are already beating, the average $[Ca^{2+}]_m$ is higher than in nonbeating cells and oscillating almost in parallel with changes in $[Ca^{2+}]_c$. In the experiments shown in Fig. 5, the average $[Ca^{2+}]_m$ was ~0.7 μM before and ~1.1 μM after addition of isoproterenol. Thus, the dehydrogenases are likely to be partially activated and able to respond much more rapidly when ATP demand is increased further by isoproterenol. Unfortunately, we could not use aequorin to give reliable estimates of resting $[Ca^{2+}]_m$, for reasons already discussed. But from other studies it appears to be in the region of 0.1–0.2 μM (16, 45), which is well below the $[Ca^{2+}]_m$ required for dehydrogenase activation (4).

Beat-to-Beat Changes in $[Ca^{2+}]_m$ in Living Cardiomyocytes—The present experiments demonstrate that mitochondrial Ca^{2+} transients can occur during a single beat in adult myocytes, although such transients are only clearly visible in the presence of β-adrenergic stimulation or supraphysiological external $[Ca^{2+}]$. Although we have shown previously, using the fluorescent indicator indo-1, that a slower rise in $[Ca^{2+}]_m$ occurs in response to an adrenergic agonist (12), we were not able to detect clear beat-to-beat changes in $[Ca^{2+}]_m$ in this earlier study. This agrees with other studies using indo-1 in rat, cat, and ferret myocytes (11, 13). However, other workers reported that $[Ca^{2+}]_m$ transients occurred in guinea pig and rabbit myocytes, using rhod-2 or fluo-3 (10, 46). So it is possible that use of different indicators, and differential loading of these dyes into cytosolic *versus* mitochondrial compartments, produces different results. Another possibility is that mitochondrial Ca^{2+} handling differs between species, as has been found for other (non-mitochondrial) Ca^{2+} transporters (47).

A further possibility is that cells in the present work were cultured for 48 h, whereas in the earlier study we used freshly isolated myocytes (12). Changes in cell morphology and loss of t-tubules have been described as early as 24 h after culture (20). However, in this study, t-tubules were still clearly present (data not shown). With regard to neonatal myocytes, our results agree with several independent studies demonstrating $[Ca^{2+}]_m$ transients in these cells, using either aequorin or the fluorescent indicator rhod-2 (15, 48, 49).

Studies from many other cell types have indicated that the subcellular organization of mitochondria is vital in determining their Ca^{2+} handling properties (16, 24). Indeed, Sharma *et al.* (50) found that in skinned myocytes application of caffeine to the cells caused a large release of Ca^{2+} from the SR that was taken up by mitochondria, as well as entering the cytosol, and the mitochondrial uptake was

inhibited by ruthenium red. Furthermore, when $[Ca^{2+}]_c$ was buffered with 1,2-bis(2-aminophenoxy)ethane-*N*,*N*,*N*′,*N*′-tetraacetic acid, an increase in $[Ca^{2+}]_m$ was still observed in mitochondria upon caffeine addition, indicating that the CaUP must be in very close proximity to the SR release channel. By using electron microscopy, the maximum distance of diffusion of Ca^{2+} from SR release channels to the mitochondrial surface has been estimated to be about 270 nm (50). Thus it is conceivable that mitochondria located in close proximity to Ca^{2+} channels on the endoplasmic reticulum/SR or plasma membrane are exposed to a much higher level of $[Ca^{2+}]$ than those elsewhere in the cytosol (51).

More recently the existence of a rapid uptake mode for Ca^{2+} has been proposed (52, 53). However, whether this represented a separate pathway or different state of the CaUP is unclear. Another recent finding proposed the existence of a ryanodine receptor in the mitochondrial membrane (54, 55). This appears to allow rapid uptake of Ca^{2+} at relatively low concentrations and so could account for physiological beat-to-beat Ca^{2+} uptake. Because this pathway is inhibited as external $[Ca^{2+}]$ increases, it could have easily been missed in earlier studies on isolated mitochondria, the majority of which used relatively high external $[Ca^{2+}]$, and indicators that were not sensitive to submicromolar $[Ca^{2+}]$. The authors suggest that as the ryanodine-sensitive pathway becomes inhibited, the classical CaUP takes over and accounts for mitochondrial Ca^{2+} uptake at higher external $[Ca^{2+}]$, and so would be the more pathologically relevant (55). It is still unclear as to whether the ryanodine receptor in the mitochondrial membrane is the same as the CaUP; they are both inhibited by RuR and Mg^{2+}, suggesting they may be the same channel. But having two separate pathways is an attractive hypothesis and would explain many of the controversies or discrepancies in the results to date.

Regulation of Cytosolic Ca^{2+} Transients by Mitochondrial Ca^{2+} Transporters?—Our observation that $[Ca^{2+}]_m$ changes during the excitation-contraction coupling cycle in the heart has implications for a role in modulating cytosolic Ca^{2+} signaling. Unfortunately, the available inhibitors of the mitochondrial CaUP, ruthenium red and Ru360, could not be used in our cells; the former is not specific, and the latter did not appear to enter cells (it had no effect on $[Ca^{2+}]_m$). However, when mitochondrial Ca^{2+} efflux was inhibited with clonazepam, mitochondrial Ca^{2+} transients were abolished, whereas $[Ca^{2+}]_m$ was maintained at levels close to those at the peak of $[Ca^{2+}]_m$ in the absence of clonazepam. This inhibitor also reduced the systolic $[Ca^{2+}]_c$ peaks, without affecting resting levels. Although our own data could not rule out an effect of clonazepam on Ca^{2+} channels of the sarcolemma or SR, others have shown this not to be the case (25–27). We also measured SR Ca^{2+} content with caffeine, and we found the results to be identical in the absence or presence of clonazepam, confirming that it is unlikely to cause a decrease in systolic $[Ca^{2+}]_c$ by depressing SR Ca^{2+} release (see Supplemental Material).

In conclusion, for the first time, we have measured both $[ATP]_c$ and $[ATP]_m$ in living cardiomyocytes and show that ATP levels respond differently to changes in ATP demand in these compartments. A possible mechanism for this effect was suggested by our observation that cardiomyocytes exhibited rapid Ca^{2+} pulses during the contractile cycle. These rapid Ca^{2+} transients are apparently decoded by the matrix dehydrogenases into a time-averaged signal that stimulates ATP production to keep pace with ATP demand, in a manner analogous to the decoding of mitochondrial Ca^{2+} transients in liver (56) and other cell types (57). Thus, stimulated mitochondria maintain a constant phosphorylation potential in the cytosol. This has been described as a "parallel activation model" (7) whereby Ca^{2+} is the key link, simultaneously stimulating ATP-consuming processes in the cytosol and ATP production in mitochondria. Classical mediators, like ATP, ADP, and P_i would also play a role, as seen in the experiments here where ATP demand is abruptly increased, and $[ATP]_m$ falls, before $[Ca^{2+}]_m$ rises to levels sufficient to activate dehydrogenases.

Acknowledgments—We thank Dr. Stephanie Choisy and Dirki Balaska for help with cell isolation and culture, Prof. Andrew Halestrap for critical comments on the manuscript, and the Medical Research Council (UK) for supporting the Bristol School of Medical Sciences Cell Imaging Facility.

REFERENCES

1. Chance, B., and Williams, G. R. (1956) *J. Biol. Chem.* **221,** 477–489
2. Brown, G. C. (1992) *Biochem. J.* **284,** 1–13
3. Katz, L. A., Swain, J. A., Portman, M. A., and Balaban, R. S. (1989) *Am. J. Physiol.* **256,** H265–H274
4. McCormack, J. G., Halestrap, A. P., and Denton, R. M. (1990) *Physiol. Rev.* **70,** 391–425
5. Das, A. M., and Harris, D. A. (1990) *Cardiovasc. Res.* **24,** 411–417
6. Territo, P. R., Mootha, V. K., French, S. A., and Balaban, R. S. (2000) *Am. J. Physiol.* **278,** C423–C435
7. Balaban, R. S. (2002) *J. Mol. Cell. Cardiol.* **34,** 1259–1271
8. Gunter, T. E., and Pfeiffer, D. R. (1990) *Am. J. Physiol.* **258,** C755–C786
9. Nicholls, D. G., and Crompton, M. (1980) *FEBS. Lett.* **111,** 261–268
10. Trollinger, D. R., Cascio, W. E., and Lemasters, J. J. (1997) *Biochem. Biophys. Res. Commun.* **236,** 738–742
11. Miyata, H., Silverman, H. S., Sollott, S. J., Lakatta, E. G., Stern, M. D., and Hansford, R. G. (1991) *Am. J. Physiol.* **261,** H1123–H1134
12. Griffiths, E. J., Stern, M. D., and Silverman, H. S. (1997) *Am. J. Physiol.* **273,** C37–C44
13. Zhou, Z., Matlib, M. A., and Bers, D. M. (1998) *J. Physiol.* (*Lond.*) **507,** 379–403
14. Bowers, K. C., Allshire, A. P., and Cobbold, P. H. (1992) *J. Mol. Cell. Cardiol.* **24,** 213–218
15. Robert, V., Gurlini, P., Tosello, V., Nagai, T., Miyawaki, A., Di Lisa, F., and Pozzan, T. (2001) *EMBO J.* **20,** 4998–5007
16. Rizzuto, R., Simpson, A. W., Brini, M., and Pozzan, T. (1992) *Nature* **358,** 325–327
17. Jouaville, L. S., Pinton, P., Bastianutto, C., Rutter, G. A., and Rizzuto, R. (1999) *Proc. Natl. Acad. Sci. U. S. A.* **96,** 13807–13812
18. Kennedy, H. J., Pouli, A. E., Ainscow, E. K., Jouaville, L. S., Rizzuto, R., and Rutter, G. A. (1999) *J. Biol. Chem.* **274,** 13281–13291
19. Ainscow, E. K., and Rutter, G. A. (2001) *Biochem. J.* **353,** 175–180
20. Mitcheson, J. S., Hancox, J. C., and Levi, A. J. (1998) *Cardiovasc. Res.* **39,** 280–300
21. Rutter, G. A., Burnett, P., Rizzuto, R., Brini, M., Murgia, M., Pozzan, T., Tavare, J. M., and Denton, R. M. (1996) *Proc. Natl. Acad. Sci. U. S. A.* **93,** 5489–5494
22. Saghir, A. N., Tuxworth, W. J., Jr., Hagedorn, C. H., and McDermott, P. J. (2001) *Biochem. J.* **356,** 557–566
23. Searle, S., Bright, N. A., Roach, T. I., Atkinson, P. G., Barton, C. H., Meloen, R. H., and Blackwell, J. M. (1998) *J. Cell Sci.* **111,** 2855–2866
24. Rutter, G. A., and Rizzuto, R. (2000) *Trends Biochem. Sci.* **25,** 215–221
25. Cox, D. A., Conforti, L., Sperelakis, N., and Matlib, M. A. (1993) *J. Cardio-*

vasc. Pharmacol. **21,** 595–599
26. Matlib, M. A., and Schwartz, A. (1983) *Life Sci.* **32,** 2837–2842
27. Matlib, M. A., Doane, J. D., Sperelakis, N., and Riccippo-Neto, F. (1985) *Biochem. Biophys. Res. Commun.* **128,** 290–296
28. Griffiths, E. J., Wei, S. K., Haigney, M. C., Ocampo, C. J., Stern, M. D., and Silverman, H. S. (1997) *Cell Calcium* **21,** 321–329
29. Brandes, R., and Bers, D. M. (2002) *Biophys. J.* **83,** 587–604
30. Ravier, M. A., and Rutter, G. A. (2005) *Diabetes* **54,** 1789–1797
31. Filippin, L., Magalhaes, P. J., Di Benedetto, G., Colella, M., and Pozzan, T. (2003) *J. Biol. Chem.* **278,** 39224–39234
32. Filippin, L., Abad, M. C., Gastaldello, S., Magalhaes, P. J., Sandona, D., and Pozzan, T. (2005) *Cell Calcium* **37,** 129–136
33. Di Lisa, F., Blank, P. S., Colonna, R., Gambassi, G., Silverman, H. S., Stern, M. D., and Hansford, R. G. (1995) *J. Physiol.* (*Lond.*) **486,** 1–13
34. Griffiths, E. J. (1999) *FEBS Lett.* **453,** 400–404
35. Katz, L. A., Koretsky, A. P., and Balaban, R. S. (1987) *FEBS Lett.* **221,** 270–276
36. Heineman, F. W., and Balaban, R. S. (1993) *Am. J. Physiol.* **264,** H433–H440
37. White, R. L., and Wittenberg, B. A. (1993) *Biophys. J.* **65,** 196–204
38. Brandes, R., and Bers, D. M. (1996) *Biophys. J.* **71,** 1024–1035
39. Eng, J., Lynch, R. M., and Balaban, R. S. (1989) *Biophys. J.* **55,** 621–630
40. Duchen, M. R., and Biscoe, T. J. (1992) *J. Physiol.* (*Lond.*) **450,** 13–31
41. Scholz, T. D., Laughlin, M. R., Balaban, R. S., Kupriyanov, V. V., and Heineman, F. W. (1995) *Am. J. Physiol.* **268,** H82–H91
42. White, R. L., and Wittenberg, B. A. (1995) *Biophys. J.* **69,** 2790–2799
43. Brandes, R., and Bers, D. M. (1997) *Circ. Res.* **80,** 82–87
44. Ingwall, J. S. (2004) *J. Mol. Cell. Cardiol.* **37,** 613–623
45. Rutter, G. A., Theler, J. M., Murgia, M., Wollheim, C. B., Pozzan, T., and Rizzuto, R. (1993) *J. Biol. Chem.* **268,** 22385–22390
46. Chacon, E., Ohata, H., Harper, I. S., Trollinger, D. R., Herman, B., and Lemasters, J. J. (1996) *FEBS Lett.* **382,** 31–36
47. Bers, D. M., Bassani, J. W., and Bassani, R. A. (1996) *Ann. N. Y. Acad. Sci.* **779,** 430–442
48. Sheu, S. S., and Jou, M. J. (1994) *J. Bioenerg. Biomembr.* **26,** 487–493
49. Huser, J., Blatter, L. A., and Sheu, S. S. (2000) *J. Bioenerg. Biomembr.* **32,** 27–33
50. Sharma, V. K., Ramesh, V., Franzini-Armstrong, C., and Sheu, S. S. (2000) *J. Bioenerg. Biomembr.* **32,** 97–104
51. Csordas, G., Thomas, A. P., and Hajnoczky, G. (2001) *Trends Cardiovasc. Med.* **11,** 269–275
52. Sparagna, G. C., Gunter, K. K., Sheu, S. S., and Gunter, T. E. (1995) *J. Biol. Chem.* **270,** 27510–27515
53. Buntinas, L., Gunter, K. K., Sparagna, G. C., and Gunter, T. E. (2001) *Biochim. Biophys. Acta* **1504,** 248–261
54. Beutner, G., Sharma, V. K., Giovannucci, D. R., Yule, D. I., and Sheu, S. S. (2001) *J. Biol. Chem.* **276,** 21482–21488
55. Beutner, G., Sharma, V. K., Lin, L., Ryu, S. Y., Dirksen, R. T., and Sheu, S. S. (2005) *Biochim. Biophys. Acta* **1717,** 1–10
56. Hajnoczky, G., Robb-Gaspers, L. D., Seitz, M. B., and Thomas, A. P. (1995) *Cell* **82,** 415–424
57. Pralong, W. F., Spat, A., and Wollheim, C. B. (1994) *J. Biol. Chem.* **269,** 27310–27314